A priori DNS development of closure for the non-linear term of the evolution equation of the conformation tensor for FENE-P fluids

P. R. Resende[1], F. T. Pinho[1,2], K. Kim[3] and R. Sureshkumar[4],

[1] Centro de Estudos de Fenómenos de Transporte, Faculdade de Engenharia Universidade do Porto, Rua Dr. Roberto Frias s/n, 4200-465 Porto, Portugal
email: resende@fe.up.pt http://www.fe.up.pt
[3] Universidade do Minho, Largo do Paço, 4704-553 Porto, Portugal
[3] Korea Institute of Energy Research, 102 Gajeong-ro, Yuseong-gu, Daejeon 305- 343, Republic of Korea
[4] The Materials Research Laboratory, Department of Energy, Environmental and Chemical Engineering, The Center for Materials Innovation, Washington University, St. Louis, MO 63130, U.S.A.

Abstract

Based on arguments of homogeneous isotropic turbulence a closure was developed to model the Reynolds average cross correlation between fluctuating conformation and rate of strain tensors appearing in the polymer stress equation of the viscoelastic fluids, dilute polymeric solution, based in FENE-P constitutive equation. The closure was calibrated against two sets of DNS data pertaining to the low Reynolds number range and the comparisons between the closure and DNS data demonstrate good agreement.

Keywords: *drag-reduction, polymer solutions, FENE-P, turbulence model, closure of* NLT_{ij}

1 Introduction

The addition of small amounts of additives that impart viscoelastic properties to fluids is an effective way to reduce drag and heat transfer as has been demonstrated extensively over the last fifty years [1]. One of the requirements for the extensive use of these viscoelastic fluids in practical engineering applications is the existence of a capability to predict accurately their flow characteristics, which so far does not exist. The DNS predictions of viscoelastic turbulent flows by Dimitropoulos et al. [2], Housiadas et al. [3] and Li et al. [4], amongst others, give insight on the physics of drag reduction (DR) by polymer additives, while providing useful data for developing adequate turbulence models. The rheological description of the dilute polymer solutions in these works was assigned to the Finitely-Extensible-Nonlinear-Elastic constitutive equation with Peterlin's approximation (FENE-P), even though some research has also been carried out with the Oldroyd-B and Giesekus models. The use of DNS for engineering calculations is prohibitively expensive and one must resort to such techniques as large-eddy simulation (LES) or Reynolds-average Navier-Stokes (RANS) methods, in their various forms. The latter method is implicitly adopted in this work and follows, with the necessary adaptations, the work developed by Pinho and co-workers [5-7] for a modified Generalized Newtonian fluid model.

In the context of single point closures, such as the $k-\varepsilon$ or second order full Reynolds stress models, the Reynolds- average evolution equation for the conformation tensor (C_{ij}) contains a new term that requires adequate closure so that the average polymer stress contribution to the turbulent momentum balance can be calculated. This new term, henceforth designated by NLT_{ij}, is the cross-correlation between the fluctuating conformation and velocity gradient tensors arising in the distortion term of Oldroyd's upper convective derivative. Additionally, Pinho et al [8] have also shown that the trace of NLT_{ij} also appears in the closure for the viscoelastic stress work appearing in the transport equations of turbulent kinetic energy and of the Reynolds stresses. Hence, an essential step in devising turbulence models for viscoelastic fluids described by the FENE-P rheological equation of state is the development of a closure for NLT_{ij}, which constitutes the aim of this work. The closure is developed from the exact equation of NLT_{ij} using both physical insight and physical arguments together with appropriate DNS data to justify some of the options and to calibrate the model coefficients. Once the model has been formulated its predictions are compared with DNS data to assess its quality. The DNS data pertains to the low drag reduction technique and are part of the large sets of data produced by Li et al [4] and Kim et al [9] for the low drag reduction regime (DR< 30%) of FENE-P fluids in fully-developed turbulent channel flow. Two sets of data are used characterized by the following parameters: a Reynolds number of $Re_{\tau 0} = 395$, a solvent to total zero-shear-rate viscosities ratio of $\beta = 0.9$ and a maximum extension $L^2 = 900$. The Weissenberg numbers are $We_{\tau 0} = 25$ and $We_{\tau 0} = 100$, corresponding to drag reductions of 18% and 37%, respectively.

The paper is organised as follows: the Reynolds-average governing equations for the turbulent flow of FENE-P fluids are presented in section 2. Section 3 derives the exact equation for the NLT_{ij} term appearing in the evolution equation of the conformation tensor that requires modelling. Then, section 4 proceeds with the development of an adequate closure for NLT_{ij} and the final form of the model is tested against the DNS data in Section 5. The paper closes with the main conclusions and recommendations for future work.

2 Governing equations and non-dimensional numbers

In what follows capital letters and overbars denote time-average quantities, whereas small letters and primes denote fluctuations. The equations are written in the indicial notation of Einstein, with $\delta_{ij} = 0$ when $i \neq j$ and $\delta_{ij} = 1$ for $i = j$. Solving a turbulent flow problem for an incompressible FENE-P fluid requires the solution of the continuity and momentum equations (1) and (2), respectively.

$$\frac{\partial U_i}{\partial x_i} = 0 \tag{1}$$

$$\rho \frac{\partial U_i}{\partial t} + \rho U_k \frac{\partial U_i}{\partial x_k} = -\frac{\partial \overline{p}}{\partial x_i} + \eta_s \frac{\partial^2 U_i}{\partial x_k \partial x_k} - \frac{\partial}{\partial x_k}\left(\rho \overline{u_i u_k}\right) + \frac{\partial \overline{\tau}_{ik,p}}{\partial x_k} \tag{2}$$

where $\overline{\tau}_{ik,p}$ is the time-averaged polymer stress, U_i is the mean velocity, $\overline{p}$ is the mean pressure, ρ is the fluid density and $-\rho\overline{u_i u_k}$ is the Reynolds stress tensor. The fluid rheology is described by the FENE-P model, where the extra stress is the sum of a Newtonian solvent contribution of viscosity η_s with a polymeric contribution, as in equation (3) below. This total extra stress has already been incorporated into the momentum equation (2).

$$\overline{\tau}_{ij} = \eta_s \left(\frac{\partial U_i}{\partial x_j} + \frac{\partial U_J}{\partial x_i} \right) + \overline{\tau}_{ij,p} \tag{3}$$

The time-averaged polymer stress $\overline{\tau}_{ij,p}$ results from Reynolds-averaging the FENE-P stress equation relating the instantaneous stress and conformation tensors and is given by equation (4). The conformation tensor (C_{ij}) is given by its Reynolds average evolution equation (5), where the first- term inside brackets on the left-hand-side is Oldroyd's upper convected derivative of C_{ij}.

$$\overline{\tau}_{ij,p} = \frac{\eta_p}{\lambda}\left[f\left(C_{kk}\right) C_{ij} - f\left(L\right)\delta_{ij} \right] + \frac{\eta_p}{\lambda} \overline{f\left(C_{kk} + c_{kk}\right) c_{ij}} \tag{4}$$

$$\left(\frac{\partial C_{ij}}{\partial t} + U_k \frac{\partial C_{ij}}{\partial x_k} - C_{jk} \frac{\partial U_i}{\partial x_k} - C_{ik} \frac{\partial U_j}{\partial x_k} \right) + \overline{u_k \frac{\partial c_{ij}}{\partial x_k}} - \left(\overline{c_{kj} \frac{\partial u_i}{\partial x_k}} + \overline{c_{ik} \frac{\partial u_j}{\partial x_k}} \right) = -\frac{\overline{\tau}_{ij,p}}{\eta_p} \tag{5}$$

The functions appearing in these equations are

$$f\left(C_{kk}\right) = \frac{L^2 - 3}{L^2 - C_{kk}} \text{ and } f\left(L\right) = 1 \tag{6}$$

As mentioned in the introduction, L^2, denotes the maximum molecular extensibility and the other parameters of the model are the relaxation time of the polymer λ and its viscosity coefficient η_p. To calculate the polymer stress it is necessary to quantify the three terms with overbars in equations (4) and (5). Housiadas et al. [3] and Li et al [4] have shown that the term $CT_{ij} = -\overline{u_k \partial c_{ij} / \partial x_k}$ is negligible in comparison with the other terms of equation (5), and Pinho et al [8] have demonstrated that it is also adequate to neglect $\overline{f\left(C_{kk} + c_{kk}\right) c_{ij}}$ in equation (4). Hence, it is only necessary to develop a closure for the term accounting for interactions between the fluctuating components of the conformation and velocity gradient tensors that originate from Oldroyd's upper convected derivative. Such term is called $NLT_{ij} = \overline{c_{kj} \frac{\partial u_i}{\partial x_k}} + \overline{c_{ik} \frac{\partial u_j}{\partial x_k}}$, following the nomenclature of [3,4].

The non-dimensional numbers appearing throughout the paper are defined as follows: the Reynolds number $Re_{\tau_0} \equiv h u_\tau / \nu_0$ is based on the friction velocity (u_τ), the channel half-height (h) and the zero shear-rate kinematic viscosity of the solution, which is the sum of the kinematic viscosities of the solvent and polymer ($\nu_0 = \nu_s + \nu_p$). The Weissenberg number is given by $We_{\tau_0} \equiv \lambda u_\tau^2 / \nu_0$ and β ($\beta \equiv \nu_s / \nu_0$) is the ratio between the solvent viscosity and the solution viscosity at zero shear rate.

3 Exact and approximate equations for NLT_{ij}

Denoting by operator $\mathcal{L}\left(\hat{C}_{kj}\right)$ the instantaneous evolution equation of $\hat{C}_{kj}$, an exact expression for NLT_{ij} was derived by Pinho [10] as $\overline{\mathcal{L}\left(\hat{C}_{kj}\right)\frac{\partial u_i}{\partial x_k}\frac{1}{f\left(\hat{C}_{mm}\right)}}+\overline{\mathcal{L}\left(\hat{C}_{ik}\right)\frac{\partial u_j}{\partial x_k}\frac{1}{f\left(\hat{C}_{mm}\right)}}$. This equation is very long and complex, so an alternative approach was suggested by Pinho [10]. It is the equation resulting from $\overline{\mathcal{L}\left(\hat{C}_{kj}\right)\frac{\partial u_i}{\partial x_k}}+\overline{\mathcal{L}\left(\hat{C}_{ik}\right)\frac{\partial u_j}{\partial x_k}}$, and the result is equation (7).

$$
\begin{aligned}
&\boxed{\overline{f\left(\ddot{C}_{mm}\right)c_{kj}\frac{\partial u_i}{\partial x_k}}+\overline{f\left(\ddot{C}_{mm}\right)c_{ik}\frac{\partial u_j}{\partial x_k}}}+C_{kj}\overline{f\left(\ddot{C}_{mm}\right)\frac{\partial u_i}{\partial x_k}}+C_{ik}\overline{f\left(\ddot{C}_{mm}\right)\frac{\partial u_j}{\partial x_k}}+\lambda\left[\overline{\frac{\partial u_i}{\partial x_k}\frac{\partial c_{kj}}{\partial t}}+\overline{\frac{\partial u_j}{\partial x_k}\frac{\partial c_{ik}}{\partial t}}\right]+\\
&+\lambda\left[\frac{\partial C_{kj}}{\partial x_n}u_n\overline{\frac{\partial u_i}{\partial x_k}}+\frac{\partial C_{ik}}{\partial x_n}u_n\overline{\frac{\partial u_j}{\partial x_k}}+\overline{\frac{\partial\left(U_n c_{kj}\right)}{\partial x_n}\frac{\partial u_i}{\partial x_k}}+\overline{\frac{\partial\left(U_n c_{ik}\right)}{\partial x_n}\frac{\partial u_j}{\partial x_k}}+u_n\overline{\frac{\partial c_{kj}}{\partial x_n}\frac{\partial u_i}{\partial x_k}}+u_n\overline{\frac{\partial c_{ik}}{\partial x_n}\frac{\partial u_j}{\partial x_k}}\right]-\\
&-\lambda\left[\frac{\partial U_k}{\partial x_n}\left(\overline{c_{jn}\frac{\partial u_i}{\partial x_k}}+\overline{c_{in}\frac{\partial u_j}{\partial x_k}}\right)+\frac{\partial U_j}{\partial x_n}\overline{c_{kn}\frac{\partial u_i}{\partial x_k}}+\frac{\partial U_i}{\partial x_n}\overline{c_{kn}\frac{\partial u_j}{\partial x_k}}+C_{kn}\left(\overline{\frac{\partial u_j}{\partial x_n}\frac{\partial u_i}{\partial x_k}}+\overline{\frac{\partial u_i}{\partial x_n}\frac{\partial u_j}{\partial x_k}}\right)\right]-\\
&-\lambda\left[C_{jn}\overline{\frac{\partial u_k}{\partial x_n}\frac{\partial u_i}{\partial x_k}}+C_{in}\overline{\frac{\partial u_k}{\partial x_n}\frac{\partial u_j}{\partial x_k}}+c_{jn}\overline{\frac{\partial u_k}{\partial x_n}\frac{\partial u_i}{\partial x_k}}+c_{in}\overline{\frac{\partial u_k}{\partial x_n}\frac{\partial u_j}{\partial x_k}}+c_{kn}\overline{\frac{\partial u_j}{\partial x_n}\frac{\partial u_i}{\partial x_k}}+c_{kn}\overline{\frac{\partial u_i}{\partial x_n}\frac{\partial u_j}{\partial x_k}}\right]=0
\end{aligned}
\tag{7}
$$

Equation (7) is exact, but does not contain directly NLT_{ij}. To obtain this quantity it is necessary to approximate the term enclosed in the rectangle as follows:

$$
\overline{f\left(\hat{C}_{mm}\right)c_{kj}\frac{\partial u_i}{\partial x_k}}+\overline{f\left(\hat{C}_{mm}\right)c_{ik}\frac{\partial u_j}{\partial x_k}}\approx f\left(C_{mm}\right)\left(\overline{c_{kj}\frac{\partial u_i}{\partial x_k}}+\overline{c_{ik}\frac{\partial u_j}{\partial x_k}}\right)=f\left(C_{mm}\right)NLT_{ij} \tag{8}
$$

This approximation is corroborated by the DNS data in Fig. 7-b) of Pinho et al [8] for some of the terms of NLT_{ij}. A reassessment for 18% drag reduction in Figure 1 (a) and for the new data at DR=37% in Figure 1(b) is not so favourable. Nevertheless, they confirm that the exact and approximate terms are proportional and can be made equal by the introduction of a coefficient. Further investigations are under way to address this issue.

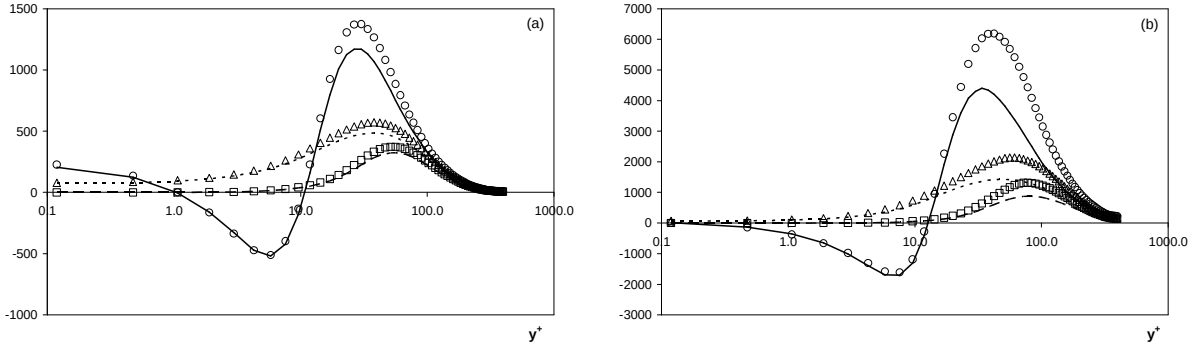

Fig.1. Comparison between the triple correlation of the fluctuations, l.h.e of eq. (8), (symbols: ○ $\overline{fc'_{1k}\,\partial u_1'/\partial x_k}$; Δ $\overline{fc'_{3k}\,\partial u_3'/\partial x_k}$ and □ $\overline{fc'_{2k}\,\partial u_2'/\partial x_k}$) and the relation of the NLTij, l.h.e of eq. (8), (lines: ── $f(C_{kk})\,NLT_{11}/2$ ─ ─ $f(C_{kk})\,NLT_{22}/2$ --- $f(C_{kk})\,NLT_{33}/2$) for the channel flow of a FENE-P with $\mathrm{Re}_\tau = 395$, $L^2 = 900$ and $\beta = 0.9$: (a) $W\mathrm{e}_\tau = 25$, DR=18%; b) $W\mathrm{e}_\tau = 100$, DR=37%.

In Fig. 2 the time-averaged trace of the conformation tensor (C_{kk}) is compared with its rms value ($\sqrt{c_{kk}^2}$) for DR= 18% and 37%. Near the walls, where the molecules are more stretched and consequently traces are larger and modify $f\left(\hat{C}_{kk}\right)$ from its equilibrium value of 1, $\sqrt{c_{kk}^2} << C_{kk}$ and consequently it is justifiable to neglect the rms in comparison with the time-average value. In the channel centreline region $\sqrt{c_{kk}^2}$ approaches C_{kk}, but both

tend to small values which do not affect $f\left(\hat{C}_{kk}\right)$, again justifying the neglect of the rms in comparison with C_{kk} when calculating $f(C_{kk})$, as found previously by Pinho et al [8]. As drag reduction increases the molecules become more stretched and Fig 1 shows that the difference in magnitudes of these two quantities increase and that on the centreline region $\sqrt{c_{kk}^2}$ remains lower than C_{kk}, further justifying the simplification. Given the form of function $f\left(\hat{C}_{kk}\right)$ this implies that its fluctuations are small and the function can come out of time-averages. A second implication is that it is justifiable to consider $\overline{f\left(\ddot{C}_{mm}\right)} \approx f\left(C_{mm}\right)$.

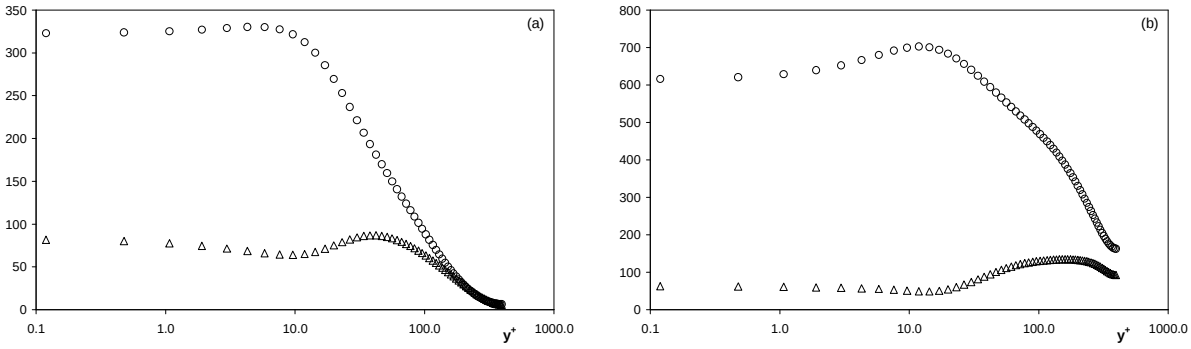

Fig.2. Transverse profiles of C_{kk} (○) and $\sqrt{\overline{c_{kk}^2}}$ (Δ) for the channel flow of a FENE-P with $\mathrm{Re}_\tau = 395$, $L^2 = 900$ and $\beta = 0.9$: (a) $W\mathrm{e}_\tau = 25$, DR=18%; b) $W\mathrm{e}_\tau = 100$, DR=37%.

4 Development of a model for NLT_{ij}

For the development of this model based on the approximately exact equation of NLT_{ij} some of the terms in equation (7) will be neglected and this is based on inspection of DNS data and physical insight. Some of the assumptions will require future confirmation on the basis of DNS data, but they are adopted here as a first approximation.

The first assumption is that terms containing the cross-correlation between velocity fluctuations and gradients of the fluctuating conformation tensor (terms like $\overline{u_n\left(\partial c_{ij}/\partial x_k\right)}$) are negligible, regardless of the indices. This is arguably correct and needs future checking, but is inspired and suggested by the neglect of term CT_{ij} by [3,4,8].

The second assumption is the use of arguments of homogeneous turbulence so that we can neglect contributions bearing similarities with terms related to the turbulent diffusion of turbulent kinetic energy. Again, this requires future confirmation, at least for some terms, and is probably valid for some other terms. Hence,

$$\overline{u_n \frac{\partial u_j}{\partial x_k}} = 0 \text{ and } \overline{u_n \frac{\partial u_i}{\partial x_k}} = 0 \tag{9}$$

Invariance laws require that convective terms are null except as part of a material derivative which is not the case here. Hence,

$$U_n \left(\overline{\frac{\partial c_{kj}}{\partial x_n}\frac{\partial u_i}{\partial x_k}} + \overline{\frac{\partial c_{ik}}{\partial x_n}\frac{\partial u_j}{\partial x_k}} \right) + \overline{u_n \frac{\partial c_{kj}}{\partial x_n}\frac{\partial u_i}{\partial x_k}} + \overline{u_n \frac{\partial c_{ik}}{\partial x_n}\frac{\partial u_j}{\partial x_k}} \approx 0 \tag{10}$$

Based on these assumptions, equation (7) simplifies to equation (11),

$$\begin{aligned} & f\left(C_{mm}\right)\overline{c_{kj}\frac{\partial u_i}{\partial x_k}} + f\left(C_{mm}\right)\overline{c_{ik}\frac{\partial u_j}{\partial x_k}} + C_{kj}\overline{f\left(\ddot{C}_{mm}\right)\frac{\partial u_i}{\partial x_k}} + C_{ik}\overline{f\left(\ddot{C}_{mm}\right)\frac{\partial u_j}{\partial x_k}} \\ & -\lambda\left[\frac{\partial U_k}{\partial x_n}\left(\overline{c_{jn}\frac{\partial u_i}{\partial x_k}} + \overline{c_{in}\frac{\partial u_j}{\partial x_k}}\right) + \frac{\partial U_j}{\partial x_n}\overline{c_{kn}\frac{\partial u_i}{\partial x_k}} + \frac{\partial U_i}{\partial x_n}\overline{c_{kn}\frac{\partial u_j}{\partial x_k}} + C_{kn}\left(\overline{\frac{\partial u_j}{\partial x_n}\frac{\partial u_i}{\partial x_k}} + \overline{\frac{\partial u_i}{\partial x_n}\frac{\partial u_j}{\partial x_k}}\right)\right] \\ & -\lambda\left[C_{jn}\overline{\frac{\partial u_k}{\partial x_n}\frac{\partial u_i}{\partial x_k}} + C_{in}\overline{\frac{\partial u_k}{\partial x_n}\frac{\partial u_j}{\partial x_k}} + c_{jn}\overline{\frac{\partial u_k}{\partial x_n}\frac{\partial u_i}{\partial x_k}} + c_{in}\overline{\frac{\partial u_k}{\partial x_n}\frac{\partial u_j}{\partial x_k}} + c_{kn}\overline{\frac{\partial u_j}{\partial x_n}\frac{\partial u_i}{\partial x_k}} + c_{kn}\overline{\frac{\partial u_i}{\partial x_n}\frac{\partial u_j}{\partial x_k}}\right] = 0 \end{aligned} \tag{11}$$

To model equation (11) we start with the four terms on the left-hand-side (l.h.s), that involve the cross-correlation between two fluctuating rates of strain and which are modelled as in Eq. (12).

$$C_{kn}\left(\overline{\frac{\partial u_j}{\partial x_n}\frac{\partial u_i}{\partial x_k}}+\overline{\frac{\partial u_i}{\partial x_n}\frac{\partial u_j}{\partial x_k}}\right)+C_{jn}\overline{\frac{\partial u_k}{\partial x_n}\frac{\partial u_i}{\partial x_k}}+C_{in}\overline{\frac{\partial u_k}{\partial x_n}\frac{\partial u_j}{\partial x_k}}\approx C_{\varepsilon_F}\frac{4}{15}\times\frac{\varepsilon}{\beta\times We_{\tau 0}\times\nu_s}C_{mm}\times f_{F2}\times\delta_{ij} \tag{12}$$

To arrive here use was made of Eq. (13), the relation between fluctuating strain rates for homogeneous isotropic turbulence [10], where λ_f is Taylor's longitudinal micro-scale. This is a length scale associated with streamwise gradients of fluctuating streamwise quantities, whereas for the gradients of cross-stream quantities Taylor's transversal length scale (λ_g) is used, which is related to λ_f by $\lambda_g^2=\lambda_f^2/2$.

$$\overline{\frac{\partial u_i}{\partial x_k}\frac{\partial u_j}{\partial x_l}}=\frac{8}{3}\frac{k}{\lambda_f^2}\left[\delta_{ij}\delta_{kl}-\frac{1}{4}\left(\delta_{ik}\delta_{jl}+\delta_{il}\delta_{jk}\right)\right] \tag{13}$$

Eq. (13) has four possible outcomes if homogeneous isotropic turbulence conditions are invoked:

$$\text{(1) when } i=j=k=l,\ \overline{\frac{\partial u_i}{\partial x_k}\frac{\partial u_j}{\partial x_l}}=\frac{4}{3}\frac{k}{\lambda_f^2} \tag{14-a}$$

$$\text{(2) when } i=j \text{ and } k=l, \text{ with } i\neq k,\ \overline{\frac{\partial u_i}{\partial x_k}\frac{\partial u_j}{\partial x_l}}=\frac{8}{3}\frac{k}{\lambda_f^2} \tag{14-b}$$

$$\text{(3) when } i=l \text{ and } k=j, \text{ with} i\neq k,\ \overline{\frac{\partial u_i}{\partial x_k}\frac{\partial u_j}{\partial x_l}}=-\frac{2}{3}\frac{k}{\lambda_f^2} \tag{14-c}$$

$$\text{(4) zero otherwise} \tag{14-d}$$

In Eq. (14) k is the turbulence kinetic energy and at high Reynolds numbers homogeneous isotropic turbulence, Taylor's longitudinal microscale is related to the dissipation of turbulent kinetic energy (ε) via Eq. (15).

$$\varepsilon=20\frac{\nu k}{\lambda_f^2} \tag{15}$$

The final outcome of these mathematical manipulations is the model of Eq. (12), where parameter C_{ε_F} was introduced to care for the modelling simplifications, whereas the damping function f_{F2} accounts for low Reynolds number effects near the wall. The quantification of the parameter and the formulation of the function were carried out against the DNS data in order to construct the best possible closure of NLT_{ij} and they are listed in Table 1.

Modelling of the term in Eq. (16) was found to be most difficult and in the end an *ad-hoc* approach was adopted as a first approximation, even though based on some physical arguments. On the one hand the cross correlation between the fluctuating conformation and strain rate tensors was decoupled as in Eq. (17), which introduced a length scale L that was taken as a viscous length scale $L\approx\nu_0/\sqrt{u_iu_m}$ for convenience. In this approach we found it convenient to use Reynolds shear stresses when modelling normal components of NLT_{ij}, so in the end the approximation of Eq. (17) transformed a second order tensor into a fourth order tensor. Hence, the remaining variables appearing in the final expression of the model must comply with symmetry and invariance properties of the original exact term and the outcome was the model on the r.h.s of Eq. (18). Other physical arguments behind the model developed for this term were considerations of increased anisotropy of the Reynolds stress and conformation tensors with drag reduction which were taken into account. In the end this modelled term did not require a damping function, simply the parameter C_{F3} that took the value listed in Table 1.

$$\frac{\partial U_k}{\partial x_n}\left(\overline{c_{jn}\frac{\partial u_i}{\partial x_k}}+\overline{c_{in}\frac{\partial u_j}{\partial x_k}}\right)+\frac{\partial U_j}{\partial x_n}\overline{c_{kn}\frac{\partial u_i}{\partial x_k}}+\frac{\partial U_i}{\partial x_n}\overline{c_{kn}\frac{\partial u_j}{\partial x_k}} \tag{16}$$

$$\frac{\partial U_j}{\partial x_n}\overline{c_{kn}\frac{\partial u_i}{\partial x_k}}:\ \frac{\partial U_j}{\partial x_n}C_{kn}\frac{\sqrt{u_iu_m}}{L} \tag{17}$$

$$\frac{\partial U_k}{\partial x_n}\left(\overline{c_{jn}\frac{\partial u_i}{\partial x_k}}+\overline{c_{in}\frac{\partial u_j}{\partial x_k}}\right)+\frac{\partial U_j}{\partial x_n}\overline{c_{kn}\frac{\partial u_i}{\partial x_k}}+\frac{\partial U_i}{\partial x_n}\overline{c_{kn}\frac{\partial u_j}{\partial x_k}}$$

$$\approx C_{F3}\times\left[\left|\frac{\partial U_j}{\partial x_k}\frac{\partial U_m}{\partial x_n}\right|C_{kn}\frac{\overline{u_i u_m}}{\nu_0\sqrt{2S_{pq}S_{pq}}}+\left|\frac{\partial U_i}{\partial x_k}\frac{\partial U_m}{\partial x_n}\right|C_{kn}\frac{\overline{u_j u_m}}{\nu_0\sqrt{2S_{pq}S_{pq}}}\right] \tag{18}$$

Invoking the previously adopted assumptions, the model for the terms containing $\overline{f\left(\ddot{\mathcal{O}}_{mm}\right)\frac{\partial u_i}{\partial x_k}}$ and $\overline{f\left(\ddot{\mathcal{O}}_{mm}\right)\frac{\partial u_j}{\partial x_k}}$ should have been zero as suggested by Eq. (19), because the time average of the fluctuating rate of strain is null.

$$C_{kj}\overline{f\left(\ddot{\mathcal{O}}_{mm}\right)\frac{\partial u_i}{\partial x_k}}\approx C_{kj}f\left(C_{mm}\right)\overline{\frac{\partial u_i}{\partial x_k}}=0 \tag{19}$$

However, there were advantages in modelling them as in Eq. (20) where the fluctuating quantities were simply substituted by time-average quantities. In retrospect this outcome is logical and is equivalent to considering that the velocity fluctuations are of the order of the mean velocity ($O(u):\ O(U)$), which is the case in the near wall region. It is also here that the mean velocity gradient, mean conformation tensor and function $f\left(C_{mm}\right)$ become larger and where the modelled term is important.

$$C_{kj}\overline{f\left(\ddot{\mathcal{O}}_{mm}\right)\frac{\partial u_i}{\partial x_k}}+C_{ik}\overline{f\left(\ddot{\mathcal{O}}_{mm}\right)\frac{\partial u_j}{\partial x_k}}\approx C_{F2}\left[C_{kj}f\left(C_{mm}\right)\frac{\partial U_i}{\partial x_k}+C_{ik}f\left(C_{mm}\right)\frac{\partial U_j}{\partial x_k}\right] \tag{20}$$

To deal with the four triple correlations we followed on the steps of classical turbulence modelling and constitutive equation modelling, where to a first approximation a nth-order correlation can be decoupled into the product of lower order correlations. Here, there was a direct transformation of all fluctuating quantities into time-averaged quantities and there was also the need to account for low Reynolds number effects via a second damping function f_{F1}.

$$\overline{c_{jn}\frac{\partial u_k}{\partial x_n}\frac{\partial u_i}{\partial x_k}}+\overline{c_{in}\frac{\partial u_k}{\partial x_n}\frac{\partial u_j}{\partial x_k}}+\overline{c_{kn}\frac{\partial u_j}{\partial x_n}\frac{\partial u_i}{\partial x_k}}+\overline{c_{kn}\frac{\partial u_i}{\partial x_n}\frac{\partial u_j}{\partial x_k}}\approx$$

$$\approx -f_{F1}\times C_{F4}\left[C_{jn}\frac{\partial U_k}{\partial x_n}\frac{\partial U_i}{\partial x_k}+C_{in}\frac{\partial U_k}{\partial x_n}\frac{\partial U_j}{\partial x_k}+C_{kn}\frac{\partial U_j}{\partial x_n}\frac{\partial U_i}{\partial x_k}+C_{kn}\frac{\partial U_i}{\partial x_n}\frac{\partial U_j}{\partial x_k}\right] \tag{21}$$

An alternative modelling of this term could have been done, based on a decoupling from the third order correlation to the product of the time-average conformation tensor with the double correlation of the fluctuating rates of deformation, so leading into a second set of terms equal to the l.h.s. of Eq. (12). This was seen to bring no advantage to the model of NLT_{ij}, and consequently the model of Eq. (19) was adopted instead.

Finally, to obtain a well- behaved model of NLT_{ij}, i.e., a model that compared well with the DNS data, there was the need to add an extra term to correct some misbehaved behaviours. This is also a situation frequently found in turbulence modelling, because the assumptions invoked often over-simplify the physics. The added term is given in Eq. (22).

$$-C_{F1}\times\frac{C_{ij}\times f(C_{mm})^2}{\lambda\times We_{\tau 0}} \tag{22}$$

Putting together all terms, the model for NLT_{ij} is

$$NLT_{ij}\equiv\overline{c_{kj}\frac{\partial u_i}{\partial x_k}}+\overline{c_{ik}\frac{\partial u_j}{\partial x_k}}\approx C_{F1}\times\frac{C_{ij}\times f(C_{mm})}{\lambda\times We_{\tau 0}}-C_{F2}\left[C_{kj}\frac{\partial U_i}{\partial x_k}+C_{ik}\frac{\partial U_j}{\partial x_k}\right]$$

$$+\frac{\lambda}{f(C_{mm})}\left[C_{F3}\times\left(\left|\frac{\partial U_j}{\partial x_k}\frac{\partial U_m}{\partial x_n}\right|C_{kn}\frac{\overline{u_i u_m}}{\nu_0\sqrt{2S_{pq}S_{pq}}}+\left|\frac{\partial U_i}{\partial x_k}\frac{\partial U_m}{\partial x_n}\right|C_{kn}\frac{\overline{u_j u_m}}{\nu_0\sqrt{2S_{pq}S_{pq}}}\right)\right]$$

$$-\frac{\lambda}{f(C_{mm})}\times f_{F1}\times C_{F4}\left[C_{jn}\frac{\partial U_k}{\partial x_n}\frac{\partial U_i}{\partial x_k}+C_{in}\frac{\partial U_k}{\partial x_n}\frac{\partial U_j}{\partial x_k}+C_{kn}\frac{\partial U_j}{\partial x_n}\frac{\partial U_i}{\partial x_k}+C_{kn}\frac{\partial U_i}{\partial x_n}\frac{\partial U_j}{\partial x_k}\right]$$

$$+\frac{\lambda}{f(C_{mm})}\left[C_{\varepsilon_F}\frac{4}{15}\times\frac{\varepsilon}{\nu_s\times\beta\times We_{\tau 0}}C_{mm}\times f_{F2}\times\delta_{ij}\right] \tag{23}$$

where the numerical values of the parameters obtained in the calibration are listed in Table 1. With the exception of C_{F3}, and less so of C_{F1}, the other parameters are of order 1, an indication of the goodness of some of the approaches used.

Table 1. Values of the model parameters and damping functions of the model *NLTij*.

C_{F1}	C_{F2}	C_{F3}	C_{F4}	C_{ε_F}
12.65	0.32	0.024	1.106	1.1275

The damping functions required to reproduce the near wall behaviour vary as usual for Newtonian fluids from zero at the wall to 1 far from the wall and are given by Eqs. (24) and (25).

$$f_{F1} = \left(1 - 0.8 \exp\left(-\frac{y^+}{30} \right) \right)^2 \tag{24}$$

$$f_{F2} = \left(1 - \exp\left(-\frac{y^+}{25} \right) \right)^4 \tag{25}$$

It is worth mentioning here that the model was initially developed and calibrated against data for 18% drag reduction. When the data for 37% drag reduction became available it was only necessary to make minor adjustments to two of the numerical coefficients, which is a good sign regarding the robustness of the model. However, both sets of data pertain to the low drag reduction regime and it remains to seen whether the model works well in the high and maximum drag reduction regimes

For the comparison of this model with DNS channel flow data under fully-developed conditions it is advantageous to present the corresponding simplified component equations. These are Eqs. (26) to (29) for NLT_{11}, NLT_{22}, NLT_{33} and NLT_{12} where indices 1, 2 and 3 indicate the streamwise, transverse an spanwise directions, respectively.

$$NLT_{11} = C_{F1} \times \frac{C_{11} \times f(C_{mm})}{\lambda \times We_{\tau 0}} - C_{F2} \left[2C_{21} \frac{\partial U_1}{\partial x_2} \right] + \frac{\lambda}{f(C_{mm})} \left[C_{F3} \times \left(2 \left| \frac{\partial U_1}{\partial x_2} \right| C_{22} \frac{\left(\overline{u_1 u_1} \right)}{\nu_0} \right) \right]$$

$$- \frac{\lambda}{f(C_{mm})} \times f_{F1} \times C_{F4} \left[2C_{22} \frac{\partial U_1}{\partial x_2} \frac{\partial U_1}{\partial x_2} \right] + \frac{\lambda}{f(C_{mm})} \left[C_{\varepsilon_F} \frac{4}{15} \times \frac{\varepsilon}{\nu_s \times \beta \times We_{\tau 0}} C_{mm} \times f_{F2} \right] \tag{26}$$

$$NLT_{22} = C_{F1} \times \frac{C_{22} \times f(C_{mm})}{\lambda \times We_{\tau 0}} + \frac{\lambda}{f(C_{mm})} \left[C_{\varepsilon_F} \frac{4}{15} \times \frac{\varepsilon}{\nu_s \times \beta \times We_{\tau 0}} C_{mm} \times f_{F2} \right] \tag{27}$$

$$NLT_{33} = C_{F1} \times \frac{C_{33} \times f(C_{mm})}{\lambda \times We_{\tau 0}} + \frac{\lambda}{f(C_{mm})} \left[C_{\varepsilon_F} \frac{4}{15} \times \frac{\varepsilon}{\nu_s \times \beta \times We_{\tau 0}} C_{mm} \times f_{F2} \right] \tag{28}$$

$$NLT_{12} = C_{F1} \times \frac{C_{12} \times f(C_{mm})}{\lambda \times We_{\tau 0}} - C_{F2} \left[C_{22} \frac{\partial U_1}{\partial x_2} \right] + \frac{\lambda}{f(C_{mm})} \left[C_{F3} \times \left(\left| \frac{\partial U_1}{\partial x_2} \right| C_{22} \frac{\left(\overline{u_1 u_2} \right)}{\nu_0} \right) \right] \tag{29}$$

5 Assessment of the performance of the model against DNS data

The model of NLT_{ij} was tested initially only against the set of data for 18% drag reduction ($We_{\tau 0} = 25$), the other parameters being $\mathrm{Re}_{\tau 0} = 395$, $L^2 = 900$ and $\beta = 0.9$. Subsequently, the 37% drag reduction data became available, corresponding to $We_{\tau 0} = 100$ the other parameters being equal, and it was only necessary to make minor adjustments to the numerical values of the coefficients in order to optimize the model. For two of the terms of the model the parameters had to be changed by a factor of 4, the ratio of Weissenberg numbers, an indication that something was missing from the original model and this was corrected. No changes were needed to the formal part of the model so these minor adjustments of the coefficients were a good sign that at least for channel flow, and in this low drag reduction regime, the present model describes well qualitatively and quantitatively the behaviour of NLT_{ij}. As will be seen next, this does not mean that there is an exact match between the DNS data and the model predictions.

Figures 2 (a) to 2-(d) compare the DNS channel flow data for the non-zero components of the NLT_{ij} tensor with the model predictions of Eqs. (26) to (29). The quantities appearing in these equations also pertain to the same two DNS data sets, so only the model for NLT_{ij} is being tested here. The quantities plotted are non-dimensional

using the normalization of the original DNS data [4]. This required the normalisation of Eqs. (26) to (29) carried out in the following way: the velocity scale is always the friction velocity, leading to the use of superscript + as in $u_i = u_i^+ u_\tau$, but for the spatial coordinates either the channel half-height ($x_i = x_i^* h$) or the viscous length are used ($x_i = x_i^+ \nu_0 / u_\tau$), leading to superscripts * and +, respectively. The two normalizations are used in the original DNS data. When mixing the two types of normalization, i.e. wall/ viscous and physical quantities, the superscript used is *, as in $NLT_{ij} = NLT_{ij}^* u_\tau / h$. Note that the ordinate scales of the figures are different in order to maximize the space available.

Careful inspection of Figure 3 shows that the model predicts better the data for DR=18% than for DR=37%. This is not surprising because the model was developed and tuned with the first set of data and essentially confirmed with the second set. No major effort at optimization in regard to both sets was carried out, as we think it is preferable at this stage to extend the model to higher drag reductions and make it general to the three drag reduction regimes than to fine tune a model which is not yet general. In assessing the model performance we must distinguish between the viscous sublayer region and the buffer and log-law regions. NLT_{ij} in the viscous sublayer is not important because the exact terms in the governing equations are much larger, as shown by Li et al [4] and Pinho et al [8]. Therefore, the discrepancies in the wall region seen in Figure 3 are essentially of no consequence. The buffer and log-law regions are those that matter and here Figure 3 shows that the model performs well. It slightly overpredicts NLT_{11} and it predicts well NLT_{22}, with a slight under-predicted location of its peak value (closer to the wall that it should). For NLT_{33} predictions are good at DR=18% but the model underpredicts at DR= 37% and for NLT_{12} the model behaves very well for DR=18% but overpredicts at DR=37%.

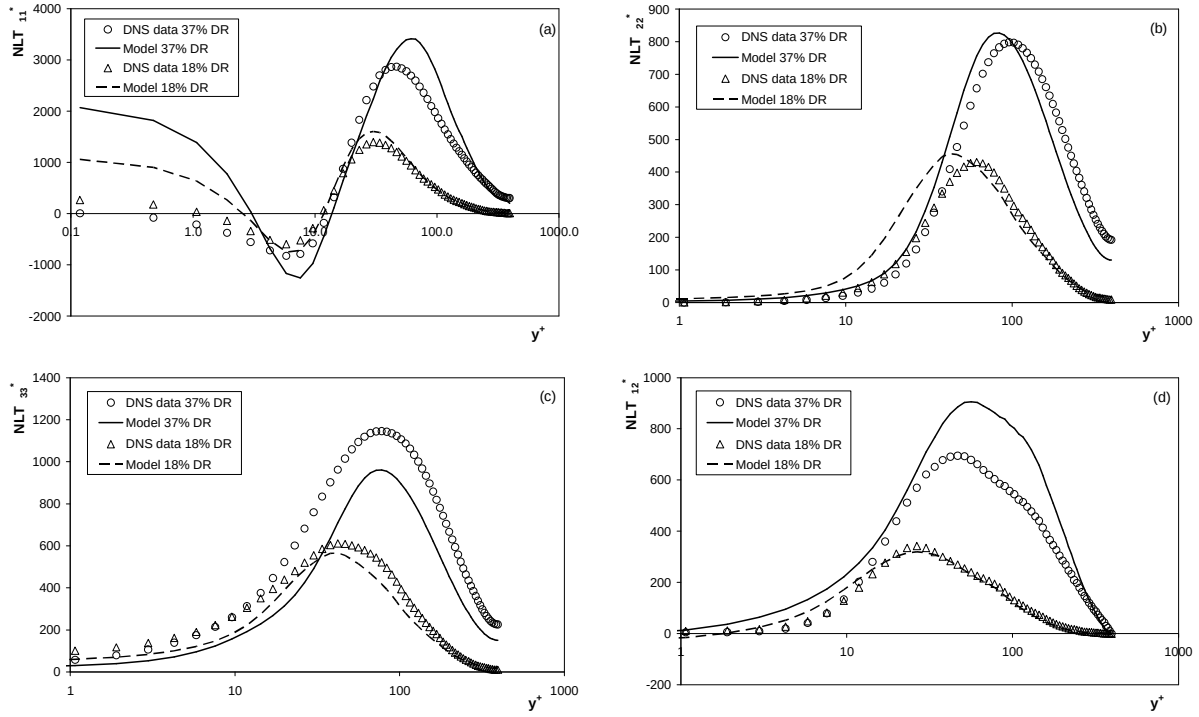

Fig.3. Comparison between the DNS data and the model for NLT_{ij} for $\mathrm{Re}_{\tau 0} = 395$, $L^2 = 900$ and $\beta = 0.9$ for $We_{\tau 0} = 25$ (18% DR) and $We_{\tau 0} = 100$ (37% DR): (a) NLT_{11}; (b) NLT_{22}; (c) NLT_{33}; (d) NLT_{12}.

As drag reduction increases, the model captures well the shift away from the wall of the peak of the various components of NLT_{ij}. In the context of a two-equation turbulence model, such as the k-ε model, the most important component of NLT_{ij} is actually NLT_{22} because this is the main term in the $\tau_{22,p}$ governing equation. In the governing equations of the other stresses, such as $\tau_{11,p}$ the other exact terms of $\tau_{11,p}$ far outweigh NLT_{11}, even though NLT_{11} is the largest component of NLT_{ij}.

Pinho et al [8] have also shown that the major impact of NLT_{ij} is not its direct contribution to the calculation of the polymer stress, but its role in the model developed for viscoelastic stress work appearing in the transport equation of turbulence kinetic energy, which relies exclusively on the trace of NLT_{ij}. Hence, in the context of a k-ε turbulence closure, it is extremely important for the model developed for NLT_{ij} to be able to predict accurately its trace, NLT_{kk}. The comparison of the DNS data and model prediction for the trace of NLT_{ij} is plotted in Figure

4. As can be seen, the quality of the predictions is better than that of NLT_{11}, the largest term of the trace by far, because the underprediction of NLT_{33} partially compensates for the overprediction of NLT_{11}.

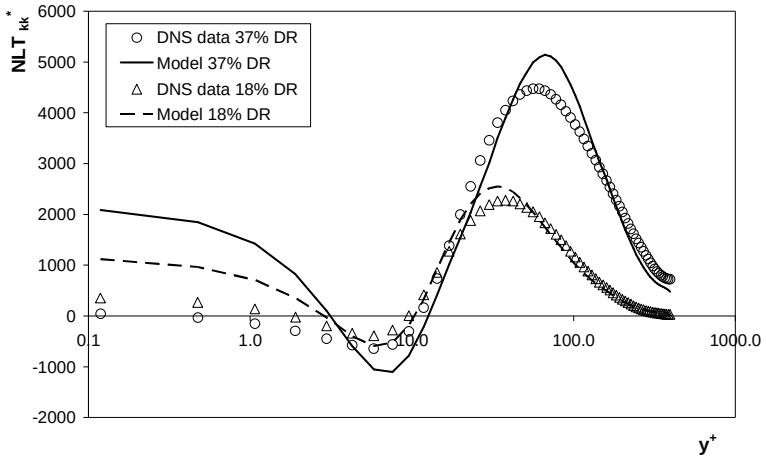

Fig.4. Comparison between the DNS data and the model for the trace of NLT_{ij} for $\mathrm{Re}_{\tau 0} = 395$, $L^2 = 900$ and $\beta = 0.9$ as a function of drag reduction: $We_{\tau 0} = 25$ (18% DR) and $We_{\tau 0} = 100$ (37% DR).

Future developments and improvements of this model are possible and should probably take into consideration the increased anisotropy of turbulent quantities as the Reynolds stress and rate of dissipation tensors, with drag reduction. The present model was developed with a clear assumption of turbulence isotropy.

6 Conclusions

Based on arguments of homogeneous isotropic turbulence a model was developed to close the Reynolds-averaged non-linear term of the polymer stress equation of dilute FENE-P fluids. This term is known as NLT_{ij} and prior to the model development the quasi-exact equation for NLT_{ij} was written down. To help the development of the closure, use was made of two sets of DNS data pertaining to channel flow of FENE-P fluids for the low drag reduction regime ($\mathrm{Re}_{\tau 0} = 395$, $L^2 = 900$ and $\beta = 0.9$ for $We_{\tau 0} = 25$ (drag reduction of 18%) and $We_{\tau 0} = 100$ (drag reduction of 37%). These data allowed first the simplification of the exact equation, by showing that some terms are negligible and later they where used to calibrate the model and quantify the parameters introduced.

The comparison between the model predictions, based on DNS data of the independent variables of the model equations (24) to (27) and the DNS data of NLT_{ij} was good. The model captured all features of the individual components of the tensor, and in particular the effects of increased drag reduction to increase the individual components of NLT_{ij} and the shift away from the wall of the location of their peak values.

The next stage is to incorporate this closure into single point RANS turbulence models in order to assess the overall behaviour of the turbulence model, which requires the development of closures for new terms appearing as a consequence of the fluid visco-elasticity and simultaneously to extend the closure of NLT_{ij} to higher drag reductions in particular in the high and maximum drag reduction regimes.

Acknowledgments

The authors gratefully acknowledge funding from FEDER and FCT through Project POCI/56342/EQU/2004 and BDR SFRH/BD/18475/2004.

References

1. J. M. J. Den Toonder, M. A. Hulsen, G. D. C. Kuiken and F. T. M. Nieuwstadt, Drag reduction by polymer additives in a turbulent pipe flow: numerical and laboratory experiments. *Journal of Fluid Mechanics*, 337, 193-231, 1997.
2. C. D. Dimitropoulos, R. Sureshkumar, A. N. Beris and R. A. Handler, Budgets of Reynolds stress, kinetic energy and streamwise enstrophy in viscoelastic turbulent channel flow. *Physics of Fluids*, 13(4), 1016-1027, 2001
3. K. D. Housiadas, A. N. Beris and R. A. Handler, Viscoelastic effects on higher order statistics and coherent structures in turbulent channel flow. *Physics of Fluids*, 17, paper 35106, 2005.

4. C. F. Li, V. K. Gupta, R. Sureshkmar and B. Khomami, Turbulent channel flow of dilute polymeric solutions: drag reduction scaling and an eddy viscosity model. *J. Non-Newt. Fluid Mech.*, 139, 177-189, 2006.
5. D. O. A. Cruz and F. T. Pinho**,** Turbulent flow predictions with a low- Reynolds number k-ε model for drag reducing fluids. *J. Non-Newt. Fluid Mech*., 114, 109-148, 2003.
6. D. O. A. Cruz, F. T. Pinho and P. R. Resende, Modelling the new stress for improved drag reduction predictions of viscoelastic pipe flow. *J. Non-Newt. Fluid Mech*, 121, 127-141, 2004.
7. P. R. Resende, M. P. Escudier, F. Presti, F. T. Pinho and D. O. A. Cruz. Numerical predictions and measurements of Reynolds normal stresses in turbulent pipe flow of polymers. *Int. J. Heat and Fluid Flow*, 27, 204-219, 2006.
8. F. T. Pinho, C. F. Li, B. A. Younis and R. Sureshkumar, A low Reynolds number k- ε turbulence model for FENE-P viscoelastic fluids. Submitted to *Journal of Non-Newtonian Fluid Mechanics*, 2007.
9. K. Kim, C. F. Li, R. Sureshkumar, S. Balachandar and R. Adrian, Effects of polymer stresses on eddy structures in drag-reduced turbulent channel flow. *J. Fluid Mech.*, 584, 281-299, 2007.
10. F. T. Pinho, Time-average double correlations in turbulence models of FENE-P viscoelastic fluids. Internal report of project FCT POCI/EQU/56342/2004, 22nd November 2005, FEUP.
11. J. Mathieu and J. Scott, *An introduction to turbulent flow.* Cambridge University Press, Cambridge, UK, 2000.